

Amplification of nanosecond pulses in a single-mode erbium-doped fluoride fibre amplifier

Nikolai B. Chichkov, Paulami Ray, Solenn Cozic, Amit Yadav, Franck Joulain, Semyon V. Smirnov, Ulf Hinze, Samuel Poulain, and Edik U. Rafailov

Abstract—We investigate the amplification of nanosecond pulses in a single-mode Er-fluoride fibre amplifier. A PPLN-based optical parametric oscillator (OPO) with a Q-switched Nd:YAG pump laser was used to generate seed pulses at a wavelength of 2790 nm. The OPO system produced seed pulses with sub-10 ns pulse durations and pulse energies of 0.5 μJ at a repetition rate of 10 kHz. These seed pulses were amplified in a single-mode Erbium-fluoride fibre amplifier, consisting of 2.2 m of double-clad fibre with a doping concentration of 7 mol%. Using this setup, we demonstrate gain values of up to 20 dB, output pulse energies of 52.7 μJ , and peak powers of more than 8 kW.

Index Terms—Mid-infrared, Fibre laser, Nanosecond pulse, Fluoride fibre, ZBLAN fibre, Erbium-doped fibre.

Laser development in the short-wavelength part of the mid-infrared (MIR) wavelength region, covering wavelengths between 2.7–3.5 μm , has accelerated in the last decade [1], [2]. Several novel laser systems have been developed and commercialised, with ongoing research and development being driven by a growing number of applications in this wavelength range [1]. The major application areas include spectroscopy [3], material processing [4], and the laser interaction with biological tissues [5].

Of particular interest for material processing, is the strong interaction of short wavelength MIR laser radiation with a range of materials. This interaction stems from the absorption properties of O-H molecular bonds, which give rise to strong absorption peaks in a variety of materials, for example in fused silica around 2.7 μm (from O-H contaminations) and at 2.93 μm in liquid water. The absorption band of O-H stretching vibrations in liquid water and biological materials covers the wavelength range of 2.7–3.1 μm . Laser radiation at these wavelengths has a penetration depth of few micrometers, enabling highly localised energy deposition for material processing applications. This creates the possibility to use high-power ns- and ps-laser sources in the short MIR for precision processing, cutting, and ablation of various materials containing O-H molecular bonds, including a variety of glasses, organics materials, and biological tissues—similar to

the processing of inorganic materials with high-power near-infrared (NIR) laser systems.

Further research and advances in material processing applications in the MIR require the development of novel high-power pulsed laser sources. To address typical requirements of high precision material processing applications, these laser sources must provide peak powers of multiple kW, pulse energies of several 10 μJ , high repetition rates (above 10 kHz), pulse durations of few nanoseconds, and diffraction limited beam profiles ($M^2 < 1.1$), to achieve sub-100 μm spatial resolution). However, the development of laser sources with the required pulse parameters and output powers still remains a challenge.

Several new types of lasers have been demonstrated and commercialised in the last decade, extending the available range of laser pulse parameters in the short MIR wavelength range [1], [2]. Among these laser systems, Er-doped fluoride fibre lasers provide the highest average output powers [6] and are currently the most promising candidates for further scaling of output powers and pulse repetition rates. Q-switched Er-doped fluoride fibre lasers provide average output powers of more than 10 W, repetition rates of 100 kHz, and pulse durations of few tens of nanoseconds [7]. Simultaneously, the use of single-mode Er-doped fibres results in diffraction limited beam-profiles [8], enabling laser applications with high spatial resolution. However, the long fibre lengths and Q-switch dynamics, which create a dependency between pulse durations and repetition rates, introduce significant limitations on achievable pulse durations. At repetition rates of few kHz, the shortest achievable pulse durations are limited to several 10 ns. Increasing the repetition rate above 100 kHz, leads to longer pulse durations of more than 100 ns [7].

An alternative approach for the design of high-power, ns-pulsed Er-doped fluoride fibre laser sources is the use of a master-oscillator power-amplifier (MOPA) configuration. In a MOPA setup, a seed laser with short pulse durations and high repetition rates is amplified in a high-gain Er-doped fluoride fibre amplifier for power scaling. Using this approach, the pulse parameters of different seed lasers—e.g. short pulse durations for OPO-systems—can be combined with the high average powers and diffraction limited beam-profiles of single-mode Er-fluoride fibre lasers. Although MOPA fibre laser systems are well established in the NIR, only few publications have investigated this approach in the MIR. Gauthier et al. [9] have demonstrated the amplification of an optical paramater generator (OPG) laser source with pulse durations of 400 ps and a repetition rate of 2 kHz in a single-mode Er-fluoride

This project has received funding from the European Union's Horizon 2020 research and innovation programme under the Marie Skłodowska-Curie grant agreement No 843801. This project has received funding from the Engineering and Physical Sciences Research Council (EPSRC), Grant No. EP/R024898/1.

N.B. Chichkov and U. Hinze are with the Institute of Quantum Optics, Leibniz University Hanover, Germany (email: n.chichkov@iqo.uni-hannover.de)

N.B. Chichkov, P. Ray, A. Yadav, and E.U. Rafailov are with the Aston Institute of Photonic Technologies, Aston University, Birmingham, UK.

U. Hinze is with the Laser nanoFab GmbH, Hanover, Germany.

S. Cozic, F. Joulain, and S. Poulain are with Le Verre Fluoré, Campus KerLann, Bruz, France.

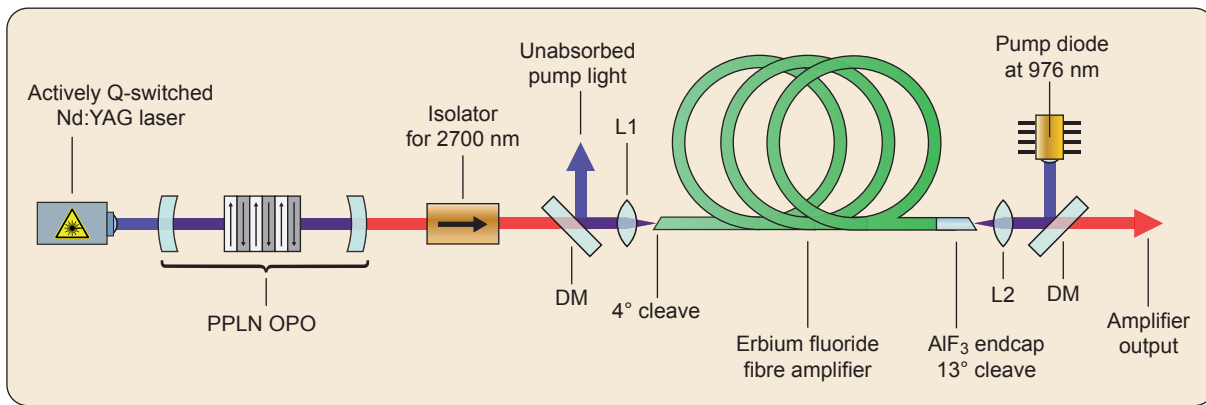


Fig. 1. Experimental setup consisting of Nd:YAG pump laser, PPLN-based OPO, and Er-doped fluoride fibre amplifier (from left to right). L1: CaF₂ lens, $f = 25$ mm; L2: CaF₂ lens, $f = 20$ mm; DM: Dichroic mirror HT at 2800 nm and HR at 980 nm.

fibre amplifier. The ps-pulses were amplified to 39 μ J (limited by the onset of self-lasing in the amplifier), which resulted in the generation of a broad supercontinuum. The demonstrated supercontinuum source is of major interest for applications in metrology and spectroscopy (as intended by the authors), but the broad wavelength range and nonlinear pulse dynamics would not be suitable for material processing applications. To investigate linear amplification of ps-pulses, i.e. without nonlinear spectral broadening, the same research group developed a multimode fluoride fibre amplifier [10]. Using a multistage amplifier with Er- and Ho-doped fibres, they demonstrated output pulses with durations of 357 ps and pulse energies of up to 122 μ J at a repetition rate of 20 kHz. The use of multimode fibres, however, resulted in a poor beam profile with an M^2 of 4.2—four times higher than single-mode fibres ($M^2 < 1.1$) and not suitable for many high precision material processing applications. Du et al. [11] have demonstrated a multimode Er-fluoride fibre amplifier with output pulse energies of 670 μ J and pulse durations of 10 ns at a low repetition rate of 10 Hz. Most recently, Aydin et al. [12] have demonstrated a dual-stage, multimode MOPA system with output pulse energies of 1 mJ, 5 kHz repetition rate, and pulse durations of 1 ns.

In this letter, we investigate the amplification of ns-pulses in a single-mode Er-fluoride fibre amplifier. To the best of our knowledge, this is the first time that the amplification of ns-pulses in a single-mode Er-fluoride fibre amplifier is demonstrated. The experimental setup of the MOPA system is illustrated in Fig. 1. The input for the fibre amplifier was obtained from the idler of a custom-made PPLN-based OPO [13], which was pumped by a Q-switched Nd:YAG laser. The seed pulses at a wavelength of 2790 nm had a pulse energy of 0.5 μ J, average power of 5.3 mW, and pulse durations of 5.2 ns (measured with photodiode rise-time of 3.5 ns) at a repetition rate of 10 kHz. The seed pulses passed through an optical isolator (Thorlabs I2700Y4, tunable isolator set to 2750 nm) and a dichroic mirror (transmission $> 97\%$ at 2800 nm, reflection $> 99.5\%$ at 980 nm), which were used to suppress back-reflections and back-propagating pump light from the fibre amplifier. Afterwards, the seed pulses were coupled with an uncoated CaF₂ lens (focal length of 25 mm) into the fibre amplifier. An overall coupling efficiency of

30 % was obtained, corresponding to a seed power of 1.6 mW inside the fibre amplifier (measured at the output). The fibre section consisted of 2.2 m of double-clad Er-doped fluoride fibre with a doping concentration of 7 mol%. We used a commercial single-mode fibre provided by Le Verre Fluoré, the same fibre as in references [6], [9]. The fibre had a core diameter of 15.5 μ m with a numerical aperture (NA) of 0.125, corresponding to a cut-off wavelength of 2.5 μ m for single-mode operation and an M^2 -value of 1.03 at 2790 nm [8]. The D-shaped pump cladding had a diameter of 260 μ m with parallel flats separated by 240 μ m and a NA of 0.46. A fluoroaluminate (AlF₃) end-cap with a length of 700 μ m was spliced to the output end of the fibre section to prevent fibre damages and degradation from O-H diffusion. The input end was left without end-cap, since the seed power of 5.3 mW was well below typically reported damage thresholds for fluoride fibres. To suppress back-reflections and self-lasing in the fibre section, the input and output facets were cleaved at 4° and 13°, respectively—the difference in angles was due to tolerances in the cleave process. The amplifier output was collimated with another uncoated CaF₂ lens (focal length of 20 mm) and passed through a second dichroic mirror.

The fibre section was pumped in counter propagating direction, using a fibre-coupled multimode pump diode (Coherent), operating at a wavelength of 978 nm with a bandwidth of 5 nm. The pump light was delivered in a multimode fibre with a core diameter of 200 μ m and NA of 0.22, collimated with an AR-coated lens (focal length 20 mm), and coupled into the output end of the fibre section through the same CaF₂ lens that was used for collimation of the amplifier output.

The temporal pulse profile of the amplified laser pulses was characterised with a fast HgCdTe photodetector (Thorlabs, PDAVJ10) with a response bandwidth of 100 MHz (at -3 dB), corresponding to a theoretical rise-time of 3.5 ns. The pulse spectra were measured with a Horiba iHR550 monochromator and an amplified PbSe-detector in combination with a lock-in amplifier. The spectra were recorded with a wavelength increment of 0.05 nm and a theoretical resolution of less than 0.2 nm, calculated for a monochromator slit size of 40 μ m. All spectra were recorded over the wavelength range from 2710 nm to 2870 nm with a signal-to-noise ratio of more

than 30 dB to ensure the absence of amplified spontaneous emission (ASE) and self-lasing in the fibre section.

Fig. 2 shows the measured output power from the amplifier at different pump powers. The threshold for amplifier gain was at a pump power of 0.5 W. Above this threshold, the output power increased linearly with a slope efficiency of 10.3 %. The maximum output power of 527 mW was reached at a pump power of 5.8 W and corresponded to a pulse energy of 52.7 μ J. We obtained a single-pass optical gain of 20 dB for the complete amplifier system (i.e. including coupling losses) and 25 dB for the fibre amplifier section without coupling losses. The optical-to-optical efficiency reached a value of 9 %—this included Fresnel reflection losses of approximately 10 % at the uncoated AlF_3 end-cap facet and the uncoated CaF_2 collimating lens. This efficiency value is in good agreement with previously reported results [9], [12].

The evolution of the amplified laser spectra at different pump powers is plotted in Fig. 3. The seed laser spectrum from the OPO was centred at 2790 nm and had a bandwidth of 9.9 nm (full-width at $1/e^2$)—the full-width at half-maximum (FWHM) had a value of 5.4 nm. The spectrum had extended, slowly decreasing side lobes (Lorentz-like shape)—3.8 % (-14 dB) of the total power was contained at wavelengths outside the main interval of 2780–2800 nm. At the output power of 40 mW, the amplified pulse spectrum was almost identical to the spectrum of the seed pulses from the OPO system with minor differences and a slightly larger bandwidth of 11.9 nm. The differences in both spectra are attributed to the fibre coupling—no nonlinear effects or ASE were observed in the amplifier at this output power level. As the output power was increased by almost one order of magnitude to 305 mW, the amplified laser spectrum began to exhibit significant changes due to nonlinearities. While the overall shape of the spectrum was preserved, the bandwidth increased to 16.0 nm and the power content of the side lobes grew to 9.6 %. Finally, Fig. 4 shows the amplified laser spectrum at the maximum output power of 527 mW. The spectrum had a bandwidth of 21.9 nm (FWHM of 7.9 nm) and 20 % (-7.0 dB) of the power was contained in the wings of the spectrum at wavelengths outside the 2780–2800 nm interval. On the logarithmic scale, we observe that the wings of the spectrum extend symmetrically over the whole wavelength range from 2690 nm to 2910 nm. The broadening of the laser spectrum and power transfer to spectral components at shorter

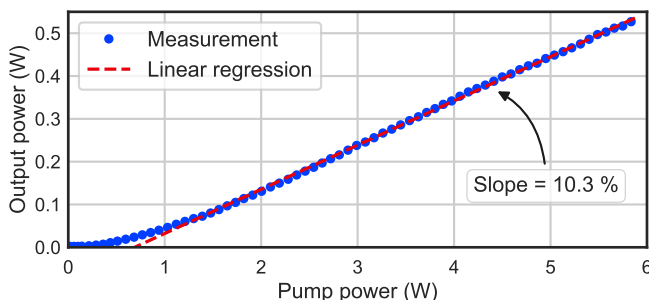


Fig. 2. Amplified output power versus launched pump power: measured values (blue) and linear regression above 1 W (red).

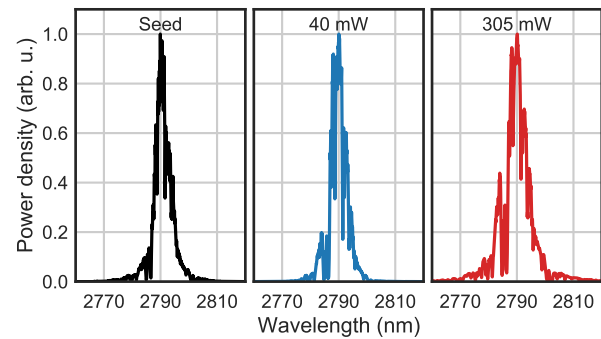


Fig. 3. Evolution of the laser spectrum during amplification: seed laser spectrum and amplified laser spectrum at output powers of 40 mW and 305 mW (from left to right).

and longer wavelengths can be attributed to nonlinear self-phase modulation (SPM) in the fibre section at peak powers of multiple kW [14]. The impact of nonlinearities can still be tolerated at the demonstrated power levels, but further power scaling, will require the investigation of mitigation measures, for example larger core diameters.

The logarithmic spectrum at the maximum output power of 527 mW showed no signs of amplified spontaneous emission or parasitic lasing (self-lasing) in the fibre section. To test for potential ASE, the fibre amplifier was operated without seed (seed laser blocked) at low pump powers. Even in this configuration, no ASE could be observed. Instead, self-lasing in the fibre section started at a pump power threshold of approximately 0.9 W (see inset of Fig. 4). This suggests that the onset of self-lasing suppresses the build-up of ASE and that self-lasing would appear before the onset of ASE—similar to the self-lasing observed in reference [9].

The temporal pulse profile and the output pulse train over 40 periods at the maximum output power of 527 mW are plotted in Fig. 5. The pulse shape and width remained almost constant during the amplification in the fibre section. We observed only minor saturation effects in the amplified pulse shape—the tail of the pulse experienced less gain than the leading part of the pulse. The measured temporal pulse profile had a full-width at half-maximum of 5.2 ns. The maximum output pulse energy of 52.7 μ J corresponded to a peak power of 8.2 kW, calculated by normalisation of the measured pulse profile. From the oscilloscope trace of the pulse train over 40 periods, we calculate a relative pulse energy fluctuation of 5.2 % (standard deviation). These fluctuations resulted from comparable pulse energy fluctuations (5.4 %) of the seed pulses generated by the OPO laser systems.

Long term stability of the presented laser system was not investigated. To avoid degradation of the fibre components, the laser system was operated only for intervals of up to 30 minutes at the maximum output power—corresponding to the time required for a full set of measurements and the recording of the optical spectrum over a span of up to 240 nm. The experiments were performed over a period of two weeks—the presented set of results was recorded at the end of this period. During that time no degradation of the laser performance or damages to fibre components

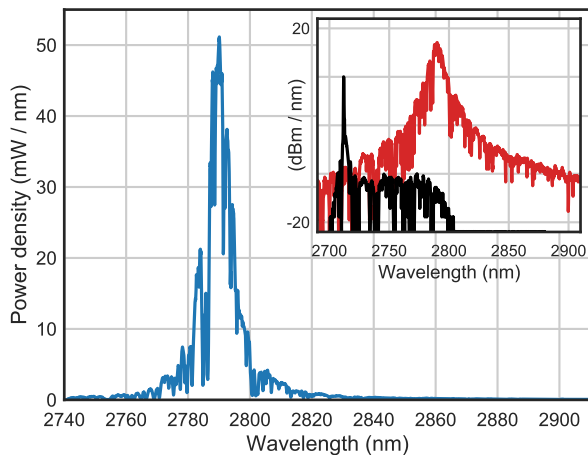


Fig. 4. Laser spectrum at the maximum output power of 527 mW, corresponding to a pulse energy of 52.7 μ J. Inset shows the amplified laser spectrum on logarithmic scale (red) and the self-lasing spectrum at 0.9 W (black).

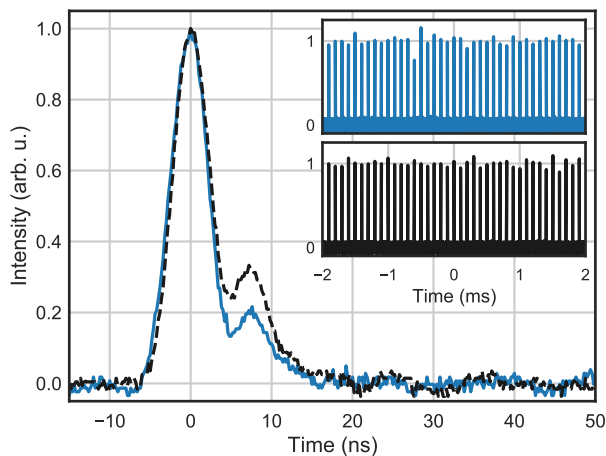


Fig. 5. Output pulse shape (HgCdTe photodiode response) at the maximum output power of 527 mW: single pulse (blue) and series of 40 successive pulses (inset, blue). Input signal from OPO: pulse shape (black, dashed) and series of 40 pulses (inset, black).

were observed. Further power-scaling beyond 52.7 μ J was also not investigated. Nonlinear effects (SPM) have already a significant impact on the output spectrum at this power level and would result in further spectral broadening at higher output powers. Additionally, the single-pass gain of the fibre amplifier of 25 dB (i.e. without coupling-losses) was approaching the threshold for self-lasing—based on reflectivity estimates for the AlF_3 end-cap and the threshold observed in reference [9]. The output power was not further increased, to avoid the onset of self-lasing and related fibre damages, i.e. the burning of the unprotected fibre facet from pulsed self-lasing.

In summary, we have demonstrated the amplification of ns-pulses in a single-mode Er-doped fluoride fibre amplifier operating at 2790 nm. We obtained output pulses with energies up to 52.7 μ J, pulse durations of 5.2 ns, and peak powers of 8.2 kW at a repetition rate of 10 kHz. To the best of our knowledge, this is the first demonstration of ns-pulse amplification in a single-mode Er-doped fluoride fibre amplifier. The use of single-mode fibres and nanosecond pulse durations en-

abled the generation of significantly higher average intensities, than have been achieved with previous Er-doped fluoride fibre amplifier systems. Comparing the output power per fibre core area with previously published setups shows an increase of almost one order of magnitude. We have achieved a value of 279 kW/cm² versus values of 41 kW/cm², 32 kW/cm², and 49 kW/cm² in references [9], [11], and [12], respectively. Building upon these results, further work will focus on power scaling, addition of amplifier stages, and improvements of amplifier efficiency. Finally, the developed Er-doped fluoride fibre amplifier can be used for the amplification of other seed laser sources in the mid-infrared, such as Cr:ZnSe lasers [2] and GaSb-based diode lasers [15], with the potential to further extend the range of laser parameters and performance of mid-infrared laser sources.

REFERENCES

- [1] S. D. Jackson and R. K. Jain, "Fiber-based sources of coherent MIR radiation: key advances and future prospects (invited)," *Optics Express*, vol. 28, no. 21, p. 30964, Oct. 2020.
- [2] S. B. Mirov, V. V. Fedorov, D. Martyshekin, I. S. Moskalev, M. Mirov, and S. Vasilyev, "Progress in Mid-IR Lasers Based on Cr and Fe-Doped II–VI Chalcogenides," *IEEE Journal of Selected Topics in Quantum Electronics*, vol. 21, no. 1, pp. 292–310, Jan. 2015.
- [3] N. Picqué and T. W. Hänsch, "Mid-IR Spectroscopic Sensing," *Optics and Photonics News*, vol. 30, no. 6, pp. 26–33, Jun. 2019.
- [4] C. Frayssinous, V. Fortin, J.-P. Bérubé, A. Fraser, and R. Vallée, "Resonant polymer ablation using a compact 3.44 μ m fiber laser," *Journal of Materials Processing Technology*, vol. 252, pp. 813–820, Feb. 2018.
- [5] M. Skorczakowski, J. Swiderski, W. Pichola, P. Nyga, A. Zajac, M. Maciejewska, L. Galecki, J. Kasprzak, S. Gross, A. Heinrich, and T. Bragagna, "Mid-infrared Q-switched Er:YAG laser for medical applications," *Laser Physics Letters*, vol. 7, no. 7, p. 498, May 2010.
- [6] Y. O. Aydin, V. Fortin, R. Vallée, and M. Bernier, "Towards power scaling of 28 μ m fiber lasers," *Optics Letters*, vol. 43, no. 18, p. 4542, Sep. 2018.
- [7] X. Zhu, G. Zhu, C. Wei, L. V. Kotov, J. Wang, M. Tong, R. A. Norwood, and N. Peyghambarian, "Pulsed fluoride fiber lasers at 3 μ m [Invited]," *Journal of the Optical Society of America B*, vol. 34, no. 3, p. A15, Mar. 2017.
- [8] H. Yoda, P. Polynkin, and M. Mansuripur, "Beam Quality Factor of Higher Order Modes in a Step-Index Fiber," *Journal of Lightwave Technology*, vol. 24, no. 3, p. 1350, Mar. 2006, publisher: IEEE.
- [9] J.-C. Gauthier, V. Fortin, S. Duval, R. Vallée, and M. Bernier, "In-amplifier mid-infrared supercontinuum generation," *Optics Letters*, vol. 40, no. 22, pp. 5247–5250, Nov. 2015.
- [10] Y. O. Aydin, V. Fortin, D. Kraemer, A. Fraser, R. Vallée, and M. Bernier, "High-energy picosecond pulses from a 2850 nm fiber amplifier," *Optics Letters*, vol. 43, no. 12, p. 2748, Jun. 2018.
- [11] W. Du, X. Xiao, Y. Cui, J. Nees, I. Jovanovic, and A. Galvanauskas, "Demonstration of 067-mJ and 10-ns high-energy pulses at 272 μ m from large core Er:ZBLAN fiber amplifiers," *Optics Letters*, vol. 45, no. 19, p. 5538, Oct. 2020.
- [12] Y. O. Aydin, Y. O. Aydin, S. Magnan-Saucier, D. Zhang, V. Fortin, D. Kraemer, R. Vallée, and M. Bernier, "Dual stage fiber amplifier operating near 3 μ m with millijoule-level, sub-ns pulses at 5 W," *Optics Letters*, vol. 46, no. 18, pp. 4506–4509, Sep. 2021.
- [13] K. A. Fedorova, A. D. McRobbie, G. S. Sokolovskii, P. G. Schunemann, and E. U. Rafailov, "Second harmonic generation in a low-loss orientation-patterned GaAs waveguide," *Optics Express*, vol. 21, no. 14, pp. 16 424–16 430, Jul. 2013.
- [14] S. Duval, M. Olivier, L.-R. Robichaud, V. Fortin, M. Bernier, M. Piché, and R. Vallée, "Numerical modeling of mid-infrared ultrashort pulse propagation in Er³⁺: fluoride fiber amplifiers," *JOSA B*, vol. 35, no. 6, pp. 1450–1462, Jun. 2018, publisher: Optical Society of America.
- [15] N. B. Chichkov, A. Yadav, E. Zherebtsov, M. Wang, G. Kipshidze, G. Belenky, L. Shterengas, and E. U. Rafailov, "Wavelength-Tunable, GaSb-Based, Cascaded Type-I Quantum-Well Laser Emitting Over a Range of 300 nm," *IEEE Photonics Technology Letters*, vol. 30, no. 22, pp. 1941–1943, Nov. 2018.